AIAA Journal
Vol. 46, No. 5, May 2008

Jet-Noise Reduction by Impinging Microjets: An Acoustic Investigation Testing Microjet Parameters

T. Castelain,* M. Sunyach,† and D. Juvé‡
Ecole Centrale de Lyon, 69134 Ecully, France
and
J.-C. Béra§
Université Claude Bernard Lyon I, 69008 Lyon, France

DOI: 10.2514/1.29411

A system of 36 impinging microjets was implemented on a round jet of Mach number 0.9, and the noise reduction was studied as a function of the microinjection mass flux, the number of microjets blowing, the layout of the blowing microjets, and the microjet diameter. Depending on the microinjection flux parameters, overall jet-noise reduction varied from 0 to 1.5 dB, showing some nonmonotonic behavior due to the change between subsonic to supersonic microjet regimes. The study of the microjet layout showed that the noise reduction decreased when the microjets were too close to each other and that certain configurations of microjet pairs could be favorable; this can be related to the flow structures induced by the microjets. Spectral analysis disclosed different control mechanisms, with high-frequency regeneration for high-injection flux, local control behavior at midfrequencies, and global behavior at low frequencies.

Nomenclature

c_0	=	sound speed under ambient conditions, m/s
D	=	main jet diameter
d	=	microjet diameter, mm
M_j	=	Mach number based on c_0
n	=	number of microjets in the main jet circumference
r_m	=	ratio between the mass flux injected by one microjet and the main jet mass flux
r_p	=	ratio between upstream pressure and atmospheric pressure
$r_p^\star$	=	value of r_p corresponding to sonic condition at the microjet nozzle exit, under the assumption of an isentropic flow
$S(f)$	=	power spectrum density of the far-field noise signal, $\mathrm{Pa}^2/\mathrm{Hz}$
St_D	=	Strouhal number based on main jet diameter D
x, y, z	=	Cartesian body axes, x designating the downstream jet axis
α	=	angle of impingement of the microjet, deg
Δ SPL	=	noise reduction provided by the control
ϕ	=	observer angle from the downstream axis

Presented as Paper 2705 at the 12th AIAA/CEAS Aeroacoustics Conference (27th AIAA Aeroacoustics Conference), Cambridge, Massachusetts, 8–10 May 2006; received 21 December 2006; revision received 8 November 2007; accepted for publication 8 December 2007.

*Ph.D., Laboratoire de Mécanique des Fluides et d'Acoustique, CNRS UMR 5509, Université Claude Bernard Lyon I, Centre Acoustique, 36, Avenue Guy de Collongue; thomas.castelain@gmail.com. Student Member AIAA.

†Professor, Laboratoire de Mécanique des Fluides et d'Acoustique, CNRS UMR 5509, Université Claude Bernard Lyon I, Centre Acoustique, 36, Avenue Guy de Collongue.

‡Professor, Laboratoire de Mécanique des Fluides et d'Acoustique, CNRS UMR 5509, Université Claude Bernard Lyon I. Senior Member AIAA.

§Professor, INSERM, 151, cours Albert Thomas, 69424 Lyon Cédex 03, France.

Introduction

Noise generation by high-speed turbulent jets remains a significant research topic due to its crucial implications for the aeronautical industry. Growing air traffic and the increasing number of airports associated with ever more restrictive regulations argue for efforts to be continued on this subject. Despite experiments and numerical simulations on jets carried out over the last few decades, the fundamental mechanisms underlying the jet noise remain to be determined. For supersonic jets, noise-generation feedback loops have been satisfactorily described [1] with good agreement between theoretic and experimental data for pure-tone noise. Jet-mixing noise, on the other hand, which occurs in both supersonic and high-subsonic jets, remains a challenge.

Considerable noise reduction was achieved by using high-bypass ratio engines in the early 1970s. Since then, considerable efforts have led to the currently implemented solution based on serrations in the nozzle exit called chevrons. Chevron effects were notably described in [2–4], with an evaluation of the thrust loss due to this passive device which provides nonnegligeable cumulative effects on long trips. To limit the thrust penalty, control systems have to be activated only when needed. Shape-memory alloy hybrid composite chevrons suggested by [5], as well as fluidic systems, meet this specification. A fluidic system made of impinging microjets was applied to supersonic jets [6–8], high-subsonic jets [9–11], and a separate flow exhaust system [12]. In this case, the benefits of such a system consist in reduced turbulence in the mixing layer and noise reduction for all angles of directivity. The magnitude of the reduction depends on the jet Mach number, M_j, and on microinjection parameters to the sensitivity of which the subtle modifications in the turbulence or noise reduction reported for high-subsonic jets [9–11] can be attributed. A parametric survey covering the range of all the previous studies is therefore of great interest, notably to determine the physical mechanisms involved in turbulence and noise reduction. The present study focused on the effect of microjet system parameters on the acoustic far field. These parameters were investigated by using different microjet configurations, varying injected mass flux, and the number, layout, and diameter of microjets.

Experimental Setup

The experiments were carried out in the anechoic facility of the Laboratoire de Mécanique des Fluides et d'Acoustique (LMFA) acoustics center (Ecole Centrale de Lyon, France). A sketch of this

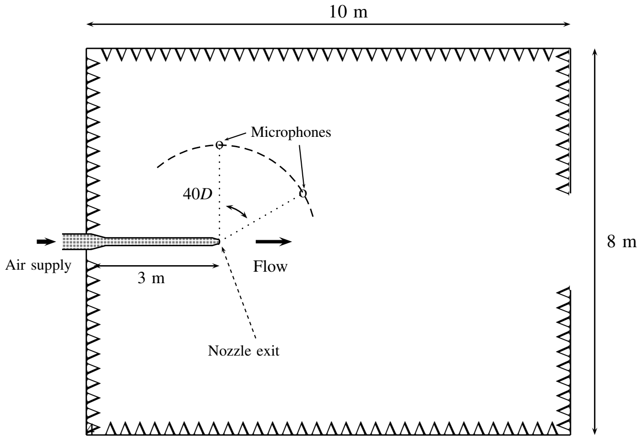

Fig. 1 Schema of the acoustic room and microphone location.

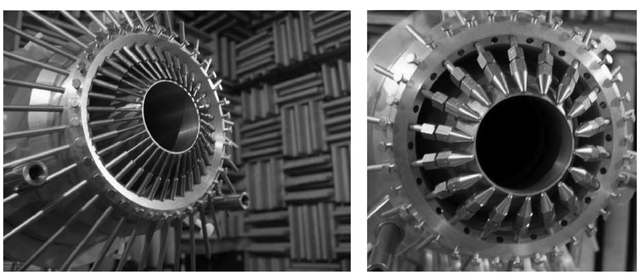

a) Typical layout with 1mm straight microjets **b) Configuration used for the study of microjet diameter d**

Fig. 2 Experimental setup.

facility and the location of the microphones are given in Fig. 1. The jet, of diameter $D = 50$ mm, was powered by a centrifugal compressor of 450 kW with a maximum mass flux of 1 $\mathrm{kg \cdot s^{-1}}$. After compression, the air was electrically heated by a set of resistances with a total power of 80 kW to maintain the temperature of the expanded jet close to room temperature. The study focused on a jet at a Mach number based on the ambient speed of sound c_0 of $M_j = 0.9$.

The control system comprised up to 36 microjets directed towards the jet centerline and impacting the jet with a 0 deg yaw angle. Two sets of microjets were used. The first comprised 36 straight brass tubes of 1 mm exit diameter (Fig. 2a). The second set comprised 18 brass tubes with removable nozzles of different diameters (Fig. 2b) and was used only to study the effect of microjet diameter. Each type of microjet was calibrated on a separate bench, measuring the total pressure and the injection mass flux. The uniformity of the microjets in terms of mass flux was checked.

The microjets were fed by a piston compressor connected to a relief valve and two pressure distributors feeding 18 microjets each. The static pressure in each distributor was monitored with a 0–60 PSI Honeywell XCA460an pressure sensor to ensure a given mass flux through the microjets.

Noise spectra were obtained with two B&K 4192 1/2 in. microphones and a B&K Nexus power supply connected to a PXI-1006 spectrum analyzer with PXI-4472 acquisition cards working at a sampling rate of $f_e = 81,920$ Hz. Spectra resulted from averaging 400 samples of 16,384 points each. Overall sound pressure levels (SPL) were computed by integrating the spectra from $f_1 = 200$ Hz to $f_2 = 35$ kHz, corresponding to a Strouhal number of $St_D = fD/Mc_0 = 0.03$–5.72, with a reference pressure of $p_{\mathrm{ref}} = 2.10^{-5}$ Pa. The microphones were located at 40 D from the nozzle exit at $\phi = 30$ deg and 90 deg, ϕ being the angle between the downstream jet axis and the microphone. These two values of ϕ enabled the characteristic behavior of jet-noise sources [1] to be illustrated.

The microjets were set at the nozzle exit, a previous study [13] having indicated that maximal noise reduction was obtained by minimizing the distance between the nozzle exit and the location of the microjet impingement on the jet-mixing layer. The microjets were set to impinge on the main jet-mixing layer with a fixed angle of $\alpha = 45$ deg, a characteristic value in the range of α tested, within which no significant differences were found. The microjets were spaced every 10 deg around the main jet circumference so that the maximum number of blowing microjets was 36. According to previous studies [13,14], the typical high-subsonic jet-noise reduction obtained with microjets is of the order of 1 to 2.5 dB, and the difference in noise reduction between two given microjet configurations is typically 0.2 dB. The parametric approach proposed here is thus relevant only if measurement repeatability is less than this typical value, which implies extreme care with regard to measurement conditions.

In the present experiments, the uncertainty (less than 2°C) associated with the jet temperature was determined by using two different thermocouples; the jet Mach number uncertainty (less than 5.10^{-3}) was estimated by monitoring static pressure and total temperature in the final duct, upstream of the nozzle exit. In studying a given parameter, one measurement of the reference jet noise was made for every three controlled jet-noise acquisitions. The standard deviation for the reference jet measurements integrated noise measurement uncertainty and the effect of variations in jet exhaust conditions. The typical standard deviation of the sound pressure level variation during one reference jet test was 0.02 dB for $\phi = 90$ deg and 0.04 dB for $\phi = 30$ deg, which perfectly meets specifications. In the controlled cases, similar measurements were made and the standard deviation was similar to or slightly higher than that for the reference jet. As the results are presented here in terms of differences in SPL, the uncertainty was consequently estimated to be less than 0.2 dB, meaning that the results may be exploited with confidence. In any case, comparison between the various configurations was based on the assumption that noise reduction was unaffected by slight changes in reference jet SPL. Note that the noise spectra measured for the injection jets alone exhibited a spectral level substantially lower than that for the main jet, whether controlled or not.

The spectra, usually presented in terms of power density spectrum $S(f)$, are given here in terms of frequency-weighted spectrum $fS(f)$ to facilitate comparison between reference and controls. Figure 3 presents the two spectrum formalisms applied to the reference jet noise validated against other reference data [15]. Figure 3b has the advantage of having linear coordinate scales enabling quick visual estimation of the frequency range contributing to the noise reduction as explained in [13]. Noise reduction in the frequency domain can then be considered by comparing the frequency-weighted spectra of the reference and controlled jets.

Effect of Injected Mass Flux

The 18 microjets used in this section are illustrated in Fig. 2a. The mass flux per microjet was varied by changing the upstream pressure by means of the pressure regulator. Monitoring the static pressure in the pressure distributor ensured a mean variation in injected mass flux during acquisition of less than 1%. The injected mass flux is considered below in terms of the ratio r_m between the mass flux injected by one microjet and the main jet mass flux.

Figure 4 gives the SPL reduction generated by the 18 microjets as a function of r_m for $\phi = 30$ deg and for $\phi = 90$ deg. For the two angles, the overall trend was towards increased SPL reduction with the mass-flux ratio; a local maximum was also observed at $r_m = 3.4 \times 10^{-4}$, followed by a local minimum at about $r_m = 5 \times 10^{-4}$, after which the SPL reduction increased monotonically with mass flux in the mass-flux range considered in the present study.

We first compared the configurations on either side of the local maximum that gave the same SPL reduction for $\phi = 30$ deg. The corresponding mass-flux ratios were $r_m^{(2)} = 2 \times 10^{-4}$ and $r_m^{(6)} = 5.6 \times 10^{-4}$, the exponent (i) denoting the corresponding point (i) in Fig. 4.

Figure 5 gives the frequency-weighted spectra $fS(f)$ corresponding to the reference jet and three values of mass-flux ratio for $\phi = 30$ deg and $\phi = 90$ deg. For $\phi = 30$ deg (Fig. 5a), the

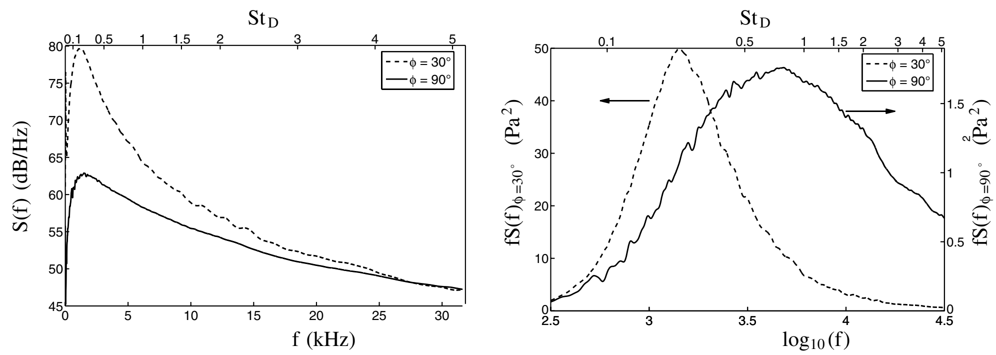

a) Power spectrum density $S(f)$ with f b) Frequency-weighted PSD $fS(f)$ with $\log_{10}(f)$

Fig. 3 Two formalisms for the representation of the power spectrum density (PSD) of the far-field noise of the reference jet, $M_j = 0.9$.

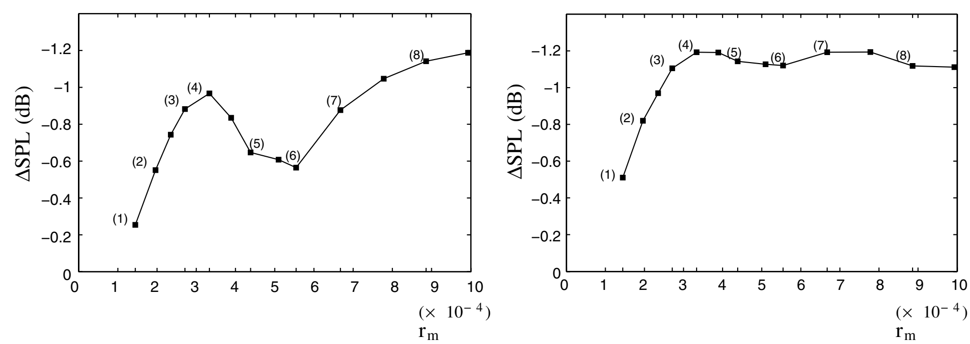

a) b)

Fig. 4 Evolution of the SPL reduction ΔSPL with the mass flux per microjet ratio r_m, a) for $\phi = 30$ deg and b) for $\phi = 90$ deg. Use of 18 1-mm-diam microjets; main jet Mach number $M_j = 0.9$.

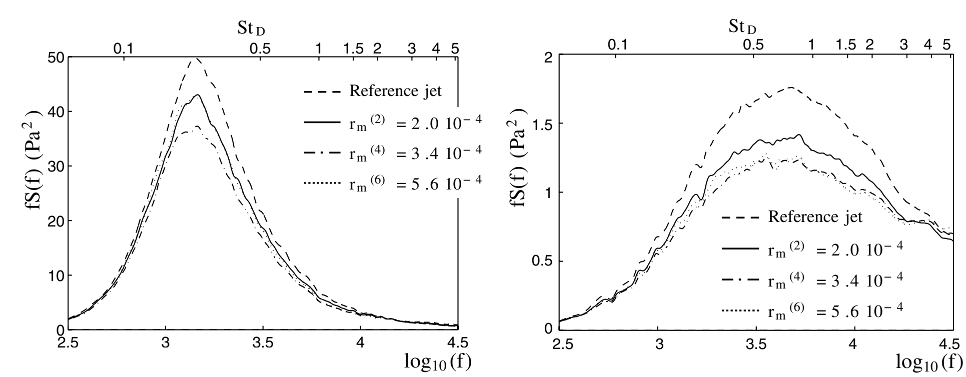

a) b)

Fig. 5 Frequency-weighted PSD of the reference jet and the controlled cases corresponding to $r_m^{(2)}$, $r_m^{(4)}$ and $r_m^{(6)}$ a) for $\phi = 30$ deg and b) for $\phi = 90$ deg. Use of 18 1-mm-diam microjets; main jet Mach number $M_j = 0.9$.

spectra for $r_m^{(2)}$ and $r_m^{(6)}$ were almost identical, particularly in the low-frequency range ($St_D < 0.5$). That this frequency range contains most of the acoustic energy explains why the SPL should be equal in the two cases. The efficiency of $r_m^{(4)}$ in comparison to $r_m^{(2)}$ or $r_m^{(6)}$ is due to greater noise reduction for $St_D < 0.5$. Careful examination of Fig. 5a indicates that in the midfrequency range ($0.5 < St_D < 2.5$) the noise reduction was slightly greater for $r_m^{(6)}$. For $\phi = 90$ deg (Fig. 5b), the SPL was largely composed of contributions from the midfrequency range for which the same trend as for $\phi = 30$ deg was observed. This explains the greater noise reduction obtained for $r_m^{(6)}$ than for $r_m^{(2)}$. Marginal noise regeneration could also be observed for $St_D > 4$ in the case $r_m^{(6)}$.

The singularity of the local maximum excepted noise reduction increased with mass-flux ratio for $\phi = 30$ deg and stagnated for $\phi = 90$ deg. Three r_m values ($r_m^{(1)}$, $r_m^{(4)}$, and $r_m^{(8)}$) illustrate this trend in Fig. 4. The corresponding spectra given in Fig. 6 reveal that the greatest spectral reduction in the low-frequency range for $\phi = 30$ deg or in the midfrequency range for $\phi = 90$ deg was achieved by the configuration with the highest mass-flux ratio ($r_m^{(8)}$). Greater noise regeneration was also observed in the high-frequency domain, in particular for $\phi = 90$ deg. This resulted from the interaction between the main jet-mixing layer and the microjets at the impact location. The early jet-mixing layer radiating high-frequency noise owing to its limited radial extension underwent profound structural modification with the use of the control, as shown by preliminary cross-field velocity measurements (Fig. 7); in particular, at high r_m values, high levels of turbulence intensities due to strong interaction between the microjets and the jet-mixing layer may have induced high-frequency noise. In this case, SPL reduction was limited for

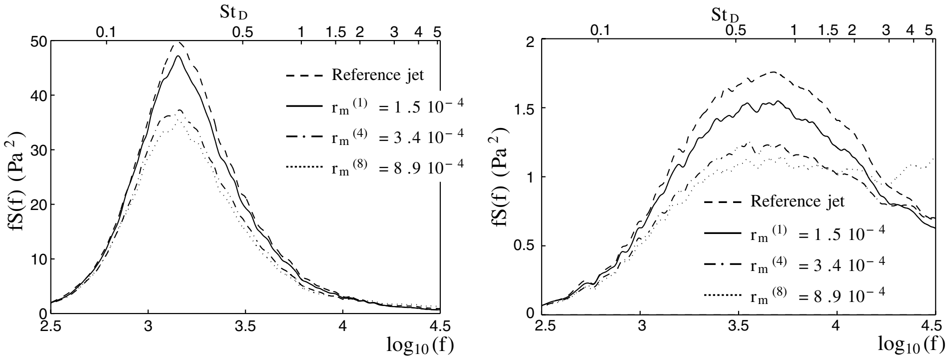

a) b)

Fig. 6 Frequency-weighted PSD of the reference jet and the controlled cases corresponding to $r_m^{(1)}$, $r_m^{(4)}$, and $r_m^{(8)}$ a) for $\phi = 30$ deg and b) for $\phi = 90$ deg. Use of 18 1-mm-diam microjets; main jet Mach number $M_j = 0.9$.

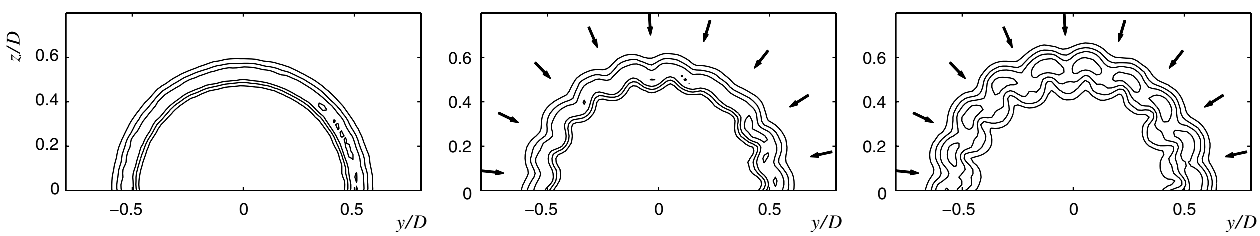

a) b) c)

Fig. 7 Contours of the mean axial turbulence intensity in the cross-plane located 1D downstream of the nozzle exit for the reference jet a), $r_m^{(2)} = 2 \times 10^{-4}$ b), and $r_m^{(8)} = 8.9 \times 10^{-4}$ c). The four contours represented correspond to 8, 11, 13.5, and 16% of the turbulence intensity $\sqrt{u'^2}/U_j$. The arrows → indicate the directions of the microjet impingement. The microjet parameters n and d are identical to those shown in Fig. 6.

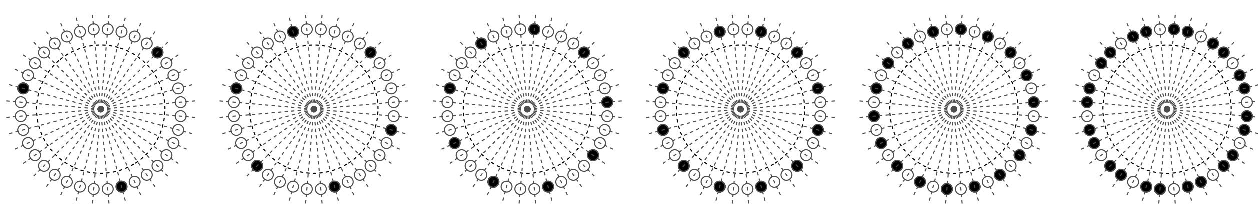

a) b) c) d) e) f)

Fig. 8 Configurations tested by varying the number of microjets. Each microjet is represented by a circle, filled if the microjet is blowing.

$r_m > r_m^{(6)}$ by a compensation between the reduction in the midfrequency range and the regeneration in the high-frequency range.

Effect of Number of Microjets

Different numbers of microjets (from 3 to 36) were tested. Figure 8 illustrates the configurations with an axisymmetric microjet distribution. The configuration in which all the microjets were blowing, not represented in Fig. 8, was also tested. The microjet diameter was 1 mm.

Figure 9a presents the evolution of SPL reduction with the number n of microjets blowing, for a mass-flux ratio $r_m^{(3)} = 2.7 \times 10^{-4}$ per microjet, with $\phi = 30$ deg and $\phi = 90$ deg. Reduction was maximal for $n = 18$, so that for $\phi = 30$ deg the configuration with $n = 36$ gave an SPL reduction very close to that obtained with $n = 6$. Moreover, the SPL reduction increased approximately linearly with the number of microjets between $n = 3$ and 18. Finally, the noise reduction obtained for $n = 9$ was of the same order of magnitude as that obtained by Alkislar et al. [10] under similar conditions (eight microjets, microjet diameter of 0.8 mm, microjet Mach number $M_j = 1.5$, main jet Mach number $M = 0.9$, yielding $r_m = 2.2 \times 10^{-4}$).

The spectra related to $n = 6$, 18, and 36 for $\phi = 30$ deg are given in Fig. 9b. This illustrates that the observed low-frequency reduction directly provided the SPL reduction shown in Fig. 9a given that most of the acoustic energy was contained in this frequency range. The spectra related to $n = 6$ and 36 were found to be almost identical. Similarly, for $\phi = 90$ deg, the low-frequency noise reductions (typically at $St_D = 0.2$) obtained with the configurations of $n = 6$ and 36 microjets were very close; in the midfrequency range, the efficiency of the configuration with $n = 36$ microjets was higher. A remarkable high-frequency noise reduction was obtained with $n = 36$ microjets, balancing the midfrequency efficiency of the configuration with $n = 18$ microjets, so that the SPL reductions given by these two configurations were very close.

The change in the noise reduction behavior for $n > 18$ correlates with the distance between two consecutive microjets. Preliminary velocity cross-field measurements, illustrated in Fig. 10, indicated that the mean velocity field was regularly corrugated for $n \leq 18$ with the corresponding spatial frequency of impingement, which was not the case for $n = 24$ or $n = 36$. In these two configurations, the excessively close microjets interacted, which may have limited impact on large-scale structures near the end of the potential core and altered the scale of generated structures affecting both low-frequency noise attenuation and high-frequency regeneration.

Figure 11 shows the evolution of SPL reduction with mass-flux ratio r_m for the entire range of n tested. The linear evolution of ΔSPL as n varied from 3 to 18, as illustrated in Fig. 9a for $r_m^{(3)} = 2.7 \times 10^{-4}$, can also be deduced from this figure for every r_m in the range

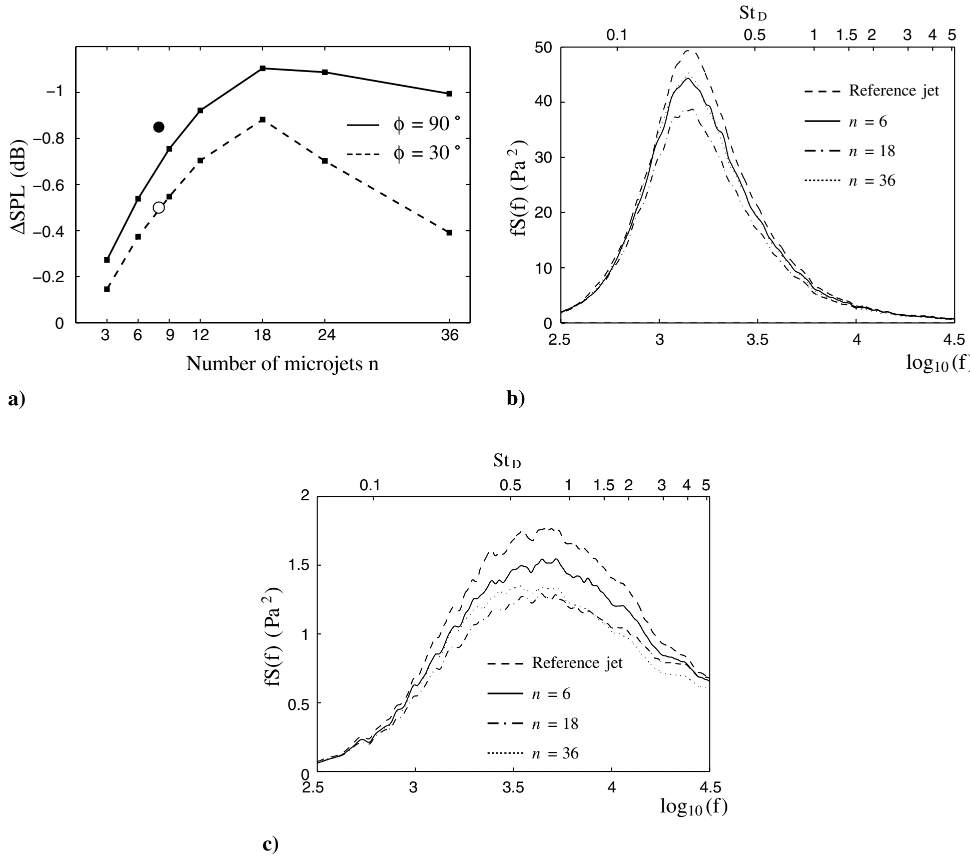

Fig. 9 Acoustic effect of the number of blowing microjets, for a mass flux per microjet ratio $r_m^{(3)} = 2.7 \times 10^{-4}$. Evolution of the SPL reduction with the number of microjets n. Results of [10] for $\phi = 90\,\mathrm{deg}$ (○) and $\phi = 30\,\mathrm{deg}$ (●) obtained in a slightly different microjet configuration are also represented a) , power spectrum densities corresponding to the reference jet and the $n = 6$, $n = 18$, and $n = 36$ cases, for $\phi = 30\,\mathrm{deg}$ b), and for $\phi = 90\,\mathrm{deg}$ c).

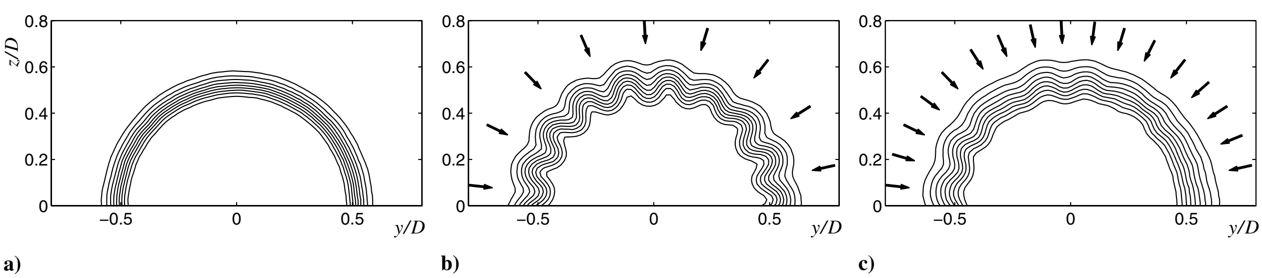

Fig. 10 Contours of the mean axial velocity, in the cross plane located 1D downstream of the nozzle exit, for the reference jet a), $n = 18$ b), and $n = 36$ c). The contours represented correspond to isovalues of the Mach number M_j from $M_j = 0.1$ to $M_j = 0.9$ by steps of 0.1. The arrows → indicate the directions of the microjet impingement. The microjet parameters r_m and d are identical to those shown in Fig. 9.

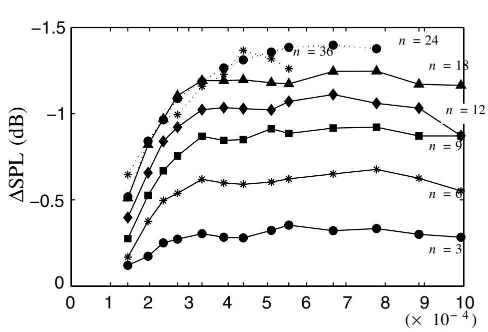

Fig. 11 Evolution of the SPL reduction at $\phi = 90\,\mathrm{deg}$ with the mass flux per microjet ratio for various numbers of blowing microjets $n = 3$ to $n = 36$.

1.5×10^{-4}–10×10^{-4}. For n above 18, more complex behavior was observed and can be attributed to interaction between consecutive microjets.

Similar trends were also observed in the evolution of noise reduction with r_m for systems of less than 18 microjets. In particular, a change in noise reduction behavior was observed at the same r_m value of $\approx 3.10^{-4}$ as described in the preceding section. Therefore, the physical mechanisms responsible for this result were not accounted for by interaction between two consecutive microjets.

Effect of Microjet Distribution

Different asymmetrical microjet layouts (see Fig. 12) were tested to investigate the directivity of the noise reduction. The number of blowing microjets could also be varied.

A first set of experiments considered the geometrical layout of the microjets with respect to the microphones. Figure 12 illustrates four positions of nine microjets with progressive rotation by $\pi/2$. In

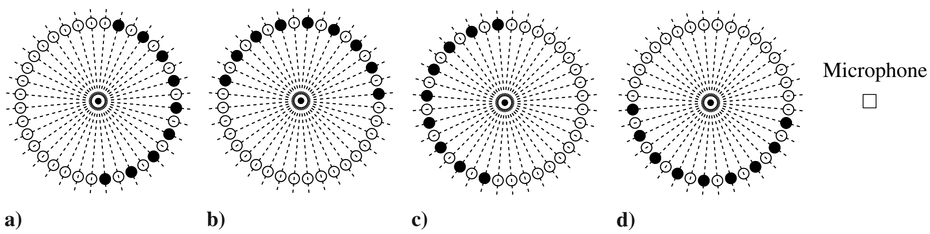

Fig. 12 Different layouts of the nine microjets relative to the microphone position.

configuration 12a, the microjets were near to and in configuration 12c away from the microphone. Treating only one part of the main jet could be considered in aeronautic applications. For example, the area treated could be the lower half of a jet on a plane during takeoff to reduce direct noise perceived on the ground.

The SPL reductions provided by the four configurations shown in Fig. 12 are given in Table 1 for angles $\phi = 30$ deg and $\phi = 90$ deg. The SPL reductions obtained were very close, the differences being below the measurement precision threshold. This was true whatever the angle of observation or injected mass-flux ratio. It can therefore be said that there was no significant directive effect in the SPL reduction provided by the microjets.

Given that there were no significant directive effects of microjet layout on SPL reduction, a second set of experiments was performed to investigate the effect of the microjet distribution within the jet circumference. Table 2 compares the mean SPL reduction provided by the four configurations of Fig. 12, and 1) by 9 (Fig. 8c) and 2) 18 equally distributed microjets (Fig. 8e). The latter configuration can be seen as the simultaneous use of the configurations 12a and 12c.

The SPL reduction obtained with the equally distributed 9-microjet configuration was larger than with the consecutive 9-microjet configuration, for all values of r_m tested, confirming the interaction effect between two consecutive microjets discussed in the preceding section. Comparing the results for the consecutive 9- and 18-microjet configurations shows that SPL reduction was doubled by doubling the number of microjets at both $\phi = 30$ deg and $\phi = 90$ deg. As all other parameters, including the distance between two consecutive microjets, remained unchanged between these two configurations, this may be taken as illustrating the additive effect on SPL reduction of the longitudinal structures generated by the microjets.

Effect of Microjet Diameter

The microjet system used in this set of experiments is illustrated in Fig. 2b. Each microjet was made of a brass tube with a threaded ending, which allowed nozzles of different diameters to be attached. This setup ensured that the geometrical settings remained unchanged between the various tests. The diameters studied were 0.7, 1, and 1.3 mm.

Figure 13a plots noise reduction against mass-flux ratio per microjet for $\phi = 30$ deg. Each curve corresponds to a given microjet diameter d. The results obtained for $\phi = 90$ deg, not represented, were identical to those for $\phi = 30$ deg. It can be observed that the SPL reduction increased overall with r_m with a local maximum, the location of which depended on the microjet diameter. It is difficult to compare the three diameters as such because the best configuration in terms of SPL reduction depended on the r_m value considered. We therefore sought a more appropriate parameter than r_m. Figure 13b plots SPL reduction against pressure ratio $r_p = \frac{p}{p_0}$ based on upstream pressure p and atmospheric pressure p_0. With the approximation of isentropic flow, the minimal value of r_p to obtain sonic conditions at the microjet exhaust was approximately $r_p^\star = 1.88$. The local maxima for the three microjet diameters considered, obtained for values of r_p around 1.5, could now be scaled; the local maximum may thus result directly from a microjet velocity effect. In particular, a transition between subsonic and supersonic microjet flow in the microjet nozzle seemed to emerge for the r_p range just below $r_p^\star$. The slight shift in the minimum observed for $d = 1.3$ mm stems from greater pressure loss upstream of the nozzle.

Comparison between the microjet diameters in terms of SPL reduction can also be seen to be more meaningful with the representation involving r_p; for a given r_p value, noise reduction increased with microjet diameter confirming the importance of mass flux per microjet for noise reduction.

Conclusions

An experimental investigation of jet-noise reduction by impinging microjets was carried out in an anechoic facility focusing on four microinjection system parameters. An optimal configuration for

Table 1 SPL reduction provided by the four configurations of Fig. 12

Configuration	SPL reduction, dB					
Related Fig. 12	$r_m^{(3)} = 2.7 \times 10^{-4}$		$r_m^{(5)} = 4.4 \times 10^{-4}$		$r_m(7) = 6.7 \times 10^{-4}$	
	30 deg	90 deg	30 deg	90 deg	30 deg	90 deg
12a	0.51	0.71	0.57	0.76	0.33	0.69
12b	0.54	0.63	0.55	0.71	0.50	0.72
12c	0.53	0.56	0.47	0.61	0.56	0.62
12d	0.47	0.60	0.45	0.68	0.50	0.63

Table 2 SPL reduction given by asymmetrical and axisymmetrical microjet configurations with $n = 9$ microjets (Figs. 12 and 8c) and $n = 18$ microjets (Fig. 8e)

Configuration	SPL reduction, dB					
(Related figure)	$r_m^{(3)} = 2.7 \times 10^{-4}$		$r_m^{(5)} = 4.4 \times 10^{-4}$		$r_m^{(7)} = 6.7 \times 10^{-4}$	
	30 deg	90 deg	30 deg	90 deg	30 deg	90 deg
9 asymmetrical (Figs. 12a–12c)	0.5	0.6	0.5	0.6	0.5	0.55
9 axisymmetrical (Fig. 8c)	0.65	0.8	0.75	1.0	1.0	0.9
18 axisymmetrical (Fig. 8e)	1.0	1.2	1.0	1.25	1.05	1.25

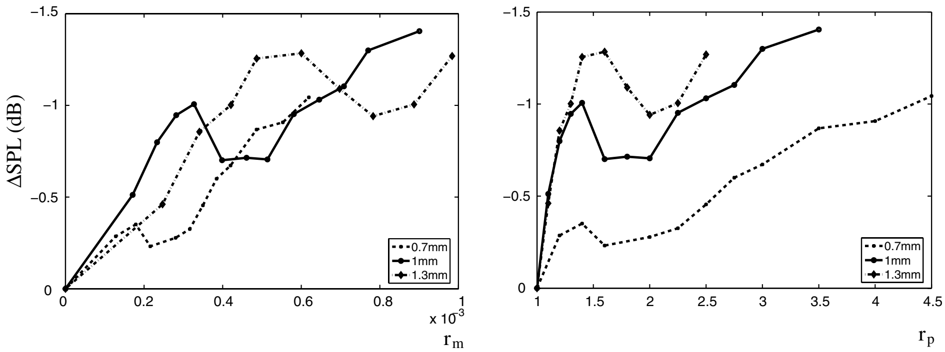

a) b)

Fig. 13 Evolution of noise reduction for $\phi = 30\,\mathrm{deg}$ with different microjet diameters: 0.7, 1, 1.3 as a function of: a) the mass-flux ratio r_m, b) the pressure ratio r_p.

noise reduction could be determined, but depended on whether control cost or noise reduction is the decisive objective. Sound pressure level reduction increased overall with injected mass flux per microjet with a local maximum emerging in this trend. Adapted scaling of the data revealed this typical behavior to be linked to flow transition from a subsonic microjet to a supersonic microjet, critical conditions being obtained at the microjet nozzle. High-injected mass-flux values were found to promote high-frequency noise generation corresponding to the interaction between the microjets and the jet-mixing layer, which is linked to the modification of the turbulence structure in the early jet development.

Modifying the microjet layout, for a given number of microjets and a given mass-flux per microjet, showed no significant azimuthal directivity of the noise reduction. An overall effect of the microjets in the low-frequency range and a local effect for higher frequencies was observed. This result should be taken into account when adapting microjets to a full-scale engine.

The maximum noise reduction was not obtained by using a maximum number of microjets because the modification of coherent structures in the flow resulted from a combination of the spacing, diameter, number, and velocity of the microjets. A characteristic dependence of noise reduction on microjet mass flux was obtained with configurations involving different numbers of blowing microjets. Configurations with paired microjets seemed to be particularly efficient. Flow measurements by stereoscopic particle image velocimetry are currently under study to investigate the formation of longitudinal structures and the dependence of microjet configurations on these structures.

References

[1] Tam, C. K. W., *Aeroacoustics of Flight Vehicles, Theory and Practice*, Vol. 1, Chap. "Jet Noise Generated by Large-Scale Coherent Motion," H. H. Hubbard, 1995, pp. 311–390.

[2] Simonich, J. C., Narayanan, S., Barber, T. J., and Nishimura, M., "Aeroacoustic Characterization, Noise Reduction and Dimensional Scaling Effects of High Subsonic Jets," *AIAA Journal*, Vol. 39, No. 11, 2001, pp. 2062–2069.

[3] Callender, B. Gutmark, E., and Martens, S., "Far-Field Acoustic Investigation into Chevron Nozzle Mechanisms and Trends," *AIAA Journal*, Vol. 43, No. 1, 2005, pp. 87–95.

[4] Saiyed, N. H., Mikkelsen, K. L., and Bridges, J. E., "Acoustics and Thrust of Quiet Separate-Flow High-Bypass-Ratio Nozzles," *AIAA Journal*, Vol. 41, No. 3, 2003, pp. 372–378.

[5] Turner, T. L., Cabell, R. H., Cano, R. J., and Fleming, G. A., "Design, Fabrication, and Testing of a SMA Hybrid Composite Jet Engine Chevron," *Proceedings of SPIE: Smart Structures and Integrated Systems*, Vol. 6173, No. 1, 2006, p. 6173B. doi:10.1117/12.660844.

[6] Greska, B., Krothapalli, A., and Arakeri, V., "A Further Investigation into the Effects of Microjets on High Speed Jet Noise," AIAA Paper 2003-3128, 2003.

[7] Greska, B., Krothapalli, A., Burnside, N., and Horne, W., "High-Speed Jet Noise Reduction Using Microjets on a Jet Engine," AIAA Paper 2004-2969, 2004.

[8] Krothapalli, A., Venkatakrishnan, L., Lourenco, L., Greska, B., and Elavarasan, R., "Turbulence and Noise Suppression of a High-Speed Jet by Water Injection," *Journal of Fluid Mechanics*, Vol. 491, No. -1, 2003, pp. 131–159. doi:10.1017/S0022112003005226

[9] Arakeri, V. H., and Krothapalli, A., "On the Use of Microjets to Suppress Turbulence in a Mach 0.9 Axisymmetric Jet," *Journal of Fluid Mechanics*, Vol. 490, No. -1, 2003, pp. 75–98. doi:10.1017/s0022112003005202

[10] Alkislar, M., Krothapalli, A., Lourenco, L., and Butler, G., "The Effect of Streamwise Vorticity on the Aeroacoustics of Mach 0.9 Axisymmetric Jet," AIAA Paper 2005-3045, 2005.

[11] Castelain, T., Béra, J. C., and Sunyach, M., "Noise Reduction of a Mach 0.7–0.9 Jet by Impinging Microjets," *Proceedings of 9th CEAS-ASC Workshop, Stockholm*, CEAS-ASC, Stockholm, 2005.

[12] Harrison, S., Gutmark, E., and Martens, S., "Jet Noise Reduction by Fluidic Injection on a Separate Flow Exhaust System," AIAA Paper 2007-439, 2007.

[13] Castelain, T., Béra, J. C., and Sunyach, M., "Noise Reduction of a Mach 0.7–0.9 Jet by Impinging Microjets," *Comptes rendus. Mécanique.*, Vol. 334, No. 2, 2006, pp. 98–104. doi:10.1016/j.crme.2006.01.001

[14] Gutmark, E., Callender, W. B., Szasz, R., Fuchs, L., and Martens, S., "Numerical Study of Fluidic Injection for Noise Reduction," *Proceedings of 9th CEAS-ASC Workshop, Stockholm*, CEAS-ASC, Stockholm, 2005.

[15] Castelain, T., "Contrôle de Jet par Microjets Impactants. Mesure de Bruit et Analyse Aérodynamique," Ph.D. Thesis, École Centrale de Lyon, Lyon, France, 2006.

E. Gutmark
Associate Editor